Shape-locking in architected materials through 3D printed magnetically activated joints

de Jong, Pier H.; Salvatori, Y.; Libonati, F.; Mirzaali, Mohammad J.; Zadpoor, Amir A.

DOI
10.1016/j.matdes.2023.112427

Publication date
2023

Document Version
Final published version

Published in
Materials and Design

Citation (APA)
de Jong, P. H., Salvatori, Y., Libonati, F., Mirzaali, M. J., & Zadpoor, A. A. (2023). Shape-locking in architected materials through 3D printed magnetically activated joints. *Materials and Design*, *235*, Article 112427. https://doi.org/10.1016/j.matdes.2023.112427

Materials & Design 235 (2023) 112427

Contents lists available at ScienceDirect

Materials & Design

journal homepage: www.elsevier.com/locate/matdes

Shape-locking in architected materials through 3D printed magnetically activated joints

Pier H. de Jong [a,1,*], Y. Salvatori [b,1], F. Libonati [b], Mohammad J. Mirzaali [a,*], Amir A. Zadpoor [a]

[a] Department of Biomechanical Engineering, Faculty of Mechanical, Maritime, and Materials Engineering, Delft University of Technology (TU Delft), Mekelweg 2, 2628 CD, Delft, the Netherlands
[b] Department of Mechanical, Energy, Transportation, and Management Engineering (DIME), University of Genoa, Genoa, Italy

ARTICLE INFO

Keywords:
Shape morphing
Locking mechanism
Kinematic fixation
Magnetism
3D printing

ABSTRACT

Shape morphing is the ability of objects to adapt to different shapes and reduce stress concentrations through increased contact area. This is a common trait of natural and engineered objects and has several applications in, among others, soft robotics and orthopedic implants. Shape morphing is achieved through flexible materials or rigid components with either kinematic or compliant joints. An additional step, namely shape locking, is needed for sustained load support. Activation of a locking mechanism can be done with any energy, among which magnetism is one. Here, we present the implementation of a magnetic locking mechanism for kinematically deformable metamaterial structures that maintain shape and support loads upon locking. The structure consists of 3D printed rigid magnetic and non-magnetic components connected by hinges. We created several prototypes of the proposed designs using two additive manufacturing methods (i.e., material extrusion and multi-material jetting) and demonstrated its application in a closed-loop grid for arbitrary shapes. Moreover, we characterized the performance of the prototypes using mechanical tests and multibody kinematic system simulations. This work highlights the viability of the locking concept and provides design considerations for future applications. Further improvement and optimizations are needed for increased efficiency and effectiveness.

1. Introduction

Shape-morphing is a crucial aspect of load support in devices working on the basis of contact, such as orthopedic implants [1,2], exosuits [3], and (soft) robotic grippers [4–7]. That is because shape morphing allows such devices to adapt to different shapes, thereby distributing loads more efficiently through increased contact area and attenuated stress concentrations. In fact, shape-morphing can be also observed in nature (e.g., in human hands and gecko toes). Shape morphing in those structures and systems can be achieved with flexible materials or through the integration of rigid components connected by kinematic or compliant joints [8]. In some cases, shape morphing should be followed by shape locking to ensure the attained shape can be preserved for further use. To achieve shape locking, a shape locking mechanism may need to be implemented in the design of the device.

The locking of shape morphing structures is also essential for sustained load support [9]. While shape morphing requires the structure to exhibit a high degree of deformability, a locked structure must retain its shape and provide sustained support while exhibiting a significant increase in its overall stiffness. Clay is an example of a material that demonstrates the ideal characteristics of both shape morphing and shape locking. In its moldable state, clay has low resistance to deformation. Once fired, however, its resistance to deformation significantly increases. Another example of locking can be seen in the human hand, where multiple muscles interact with each other to lock the hand into a specific shape. In tandem, these structural elements enable the adaptation of the shape morphing structure and the application of gripping force to an object.

The primary challenge when combining shape morphing with shape locking in one single mechanism lies in the fact that these two steps often have contradictory design requirements. For example, while many degrees of freedom (DoF) are essential for shape morphing, it complicates the locking of the structure in the acquired shape. In this context, it is important to realize that while shape morphing and shape locking are interdependent processes, the mechanism that induces the shape adaptation often also locks the structure in a particular configuration. That is

* Corresponding authors.
E-mail addresses: p.h.dejong@tudelft.nl (P.H. de Jong), m.j.mirzaali@tudelft.nl (M.J. Mirzaali).
[1] These authors contributed equally.

https://doi.org/10.1016/j.matdes.2023.112427
Received 19 April 2023; Received in revised form 12 October 2023; Accepted 23 October 2023
Available online 28 October 2023

partially because having two separate mechanisms for shape morphing and shape locking can highly complicate the design and fabrication of such structures. Another route to resolve the contradictory design requirements is to apply different working principles in the same structure for shape morphing and shape locking. The activation energy required for morphing and locking can take various forms, including mechanical [9], chemical [10], thermal [11–18], pneumatic [19], or (electro)magnetic [20–28]. Any combinations of these mechanisms can be utilized for shape morphing and shape locking. For instance, light can be used to alter the chemical composition, heat can be employed to control a mechanical system [29], magnetism can be utilized to both heat and deform a structure [30–32] or mechanically block a joint [33]. The activation energy is crucial for achieving the desired shape morphing properties [6,7,26], such as locality [13], reversibility [27,34] and continuity [35].

In this work, we examine the shape morphing and locking of structures in a kinematic metamaterial concept, also referred to as the "metallic clay" [8]. Kinematic metamaterials are a type of metamaterial [36,37] composed of rigid components connected by movable joints and are capable of kinematic deformations. The shape morphing and locking of these structures can be independently controlled, offering a wide range of potential applications. To lock the structure, the joints need to be restricted in their motion, which can be accomplished by enhancing their stiffness through deployment and multi-stability [38,39]. When the stiffness is significantly increased, one may consider the structure to have been locked. The complete elimination of the DoF of a joint or the entire system is, however, only achieved through a locking process [35]. The DoF determine the number of possible transforms that an object can undergo. In the case of kinematically deformable structures, there is a large but finite number of DoF. To fully lock the shape of such a structure, all these DoF must be eliminated, requiring both a locking principle and an activation method.

The aim of this study is to explore the fundamentals of locking of kinematically deformable structures [8] and to propose an approach based on magnetic force for contactless accomplishment of this task in an otherwise purely mechanical structure. We focus on an in-plane deforming design that has multiple DoF and can be transformed into various shapes through mechanical manipulation (Fig. 1). We designed and implemented a locking mechanism that can be triggered to lock the shape in place. A multibody kinematic system approach was used and expanded upon to numerically simulate the morphing behavior of the system upon locking individual elements. Eventually, the conceptual design is 3D printed using two different additive manufacturing (AM) techniques and is evaluated using mechanical tests. The unit cells of these structures are designed such that they can be locked individually through mechanical activation through magnetic forces. This study, therefore, aims at providing: i) an in-depth understanding of the challenges in locking shape-morphing, kinematically-deformable structures, and ii) a tangible demonstration of a magnetically-activated locking mechanism that can be utilized to control the shape of a kinematically-deformable structure. Although the interlocking latch mechanism is a classic type of mechanism often used in mechanical systems, the methodology of its implementation in this study presents valuable new insights.

2. Materials and methods

To investigate the challenges associated with the locking of shape morphing mechanisms, we examined an existing in-plane deforming kinematic design [8] and modified it to incorporate a reversible, magnetically-activated locking mechanism. The design consisted of a network of rigid bodies and hinged struts, which provided the structure with multiple DoF. These DoF are selectively locked in groups of four at the scale of individual bodies by applying a magnetic field. The locking can be reversed to an unlocked state by redirecting the magnetic field. By using magnetism as the activation method, the internal locking mechanism can be triggered from outside of the structure without the need for physical contact with the moving parts. The shape-morphing and locking mechanism were implemented in two distinct designs: a modular design and a semi-non-assembly design.

2.1. Design and working principles

All the designs shared the same principle of locking as well as the same key dimensions. A translating ring is moved by magnetism to interlock with the connected struts and constrain their rotation. Depending on the type of application, one can introduce a "snapping" mechanism to keep the lock in place after the magnetic stimulus is removed. With this principle, two distinct designs were created: a modular design and a semi-non-assembly design.

The first (colored primarily white) design of the proposed structure features modular components that can be connected via struts for the ease of assembly and experimentation (Fig. 2a). The parts were manufactured using MEX-TRB/P [40], as detailed in Table 1. Each component is equipped with four revolute joints, which are locked using a central ring made of an iron composite material that is attracted to magnetism (Fig. 2b). The ring can be positioned and snapped into place by using a magnetic field. This design features simple components that can be

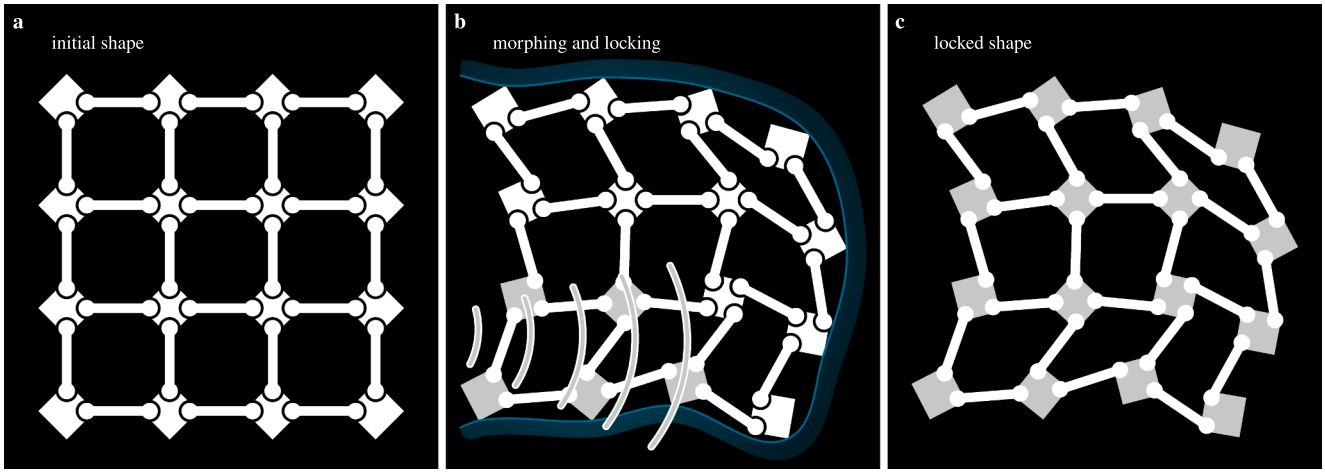

Fig. 1. An illustration of the shape morphing and shape locking principles using an in-plane deforming structure. a) The structure is equipped with multiple hinges that provide multiple DoF. b) The structure is transformed into a desired shape and a stimulus is applied to lock the hinges in place. c) The locked structure retains its shape even after being removed from the target shape.

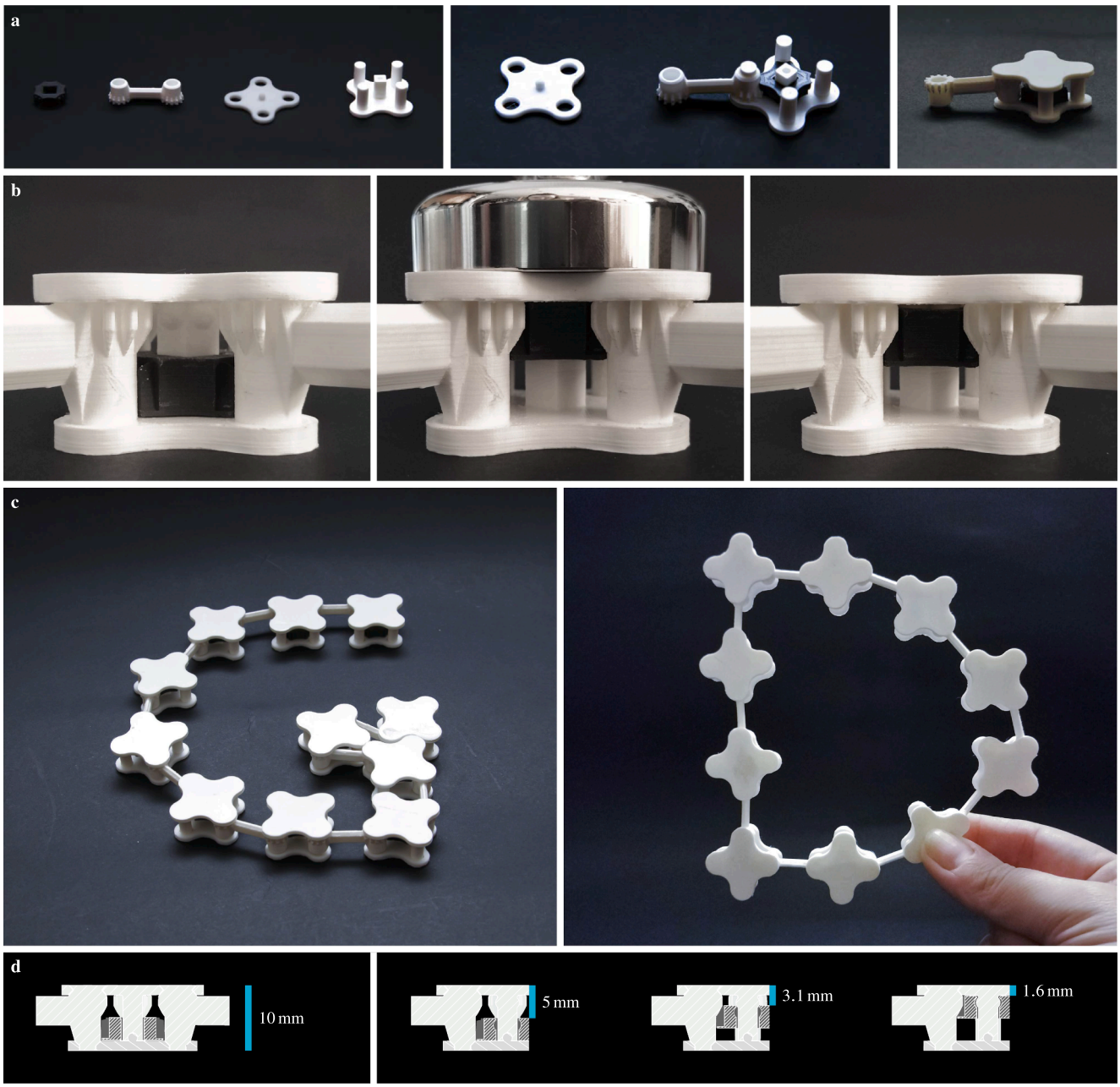

Fig. 2. An illustration of the design and functionality of the magnetic locking of a shape morphing mechanism. a) The 3D-printed components included the iron-PLA composite locking ring (grey), connecting struts (white PLA), and body pieces (white PLA). The ring and struts were placed on one of the body pieces. The full assembly with one unit of each component has a single transforming DoF (excluding the ring's translation). b) In the unlocked state, the ring is down and does not engage with the teeth on the struts, allowing them to rotate. The placement of a magnet on top shifts the ring upward and locks the struts in place, removing the DoF. The design presented here ensures that the ring remains "snapped" in place and remains locked when the magnet is removed. c) Combining unit cells creates a structure that can be locked in a desired shape. We demonstrate an open-loop and a closed-loop structure. d) The cross-sections of the main elements for a non-assembly development of the design with the dimension of all the implementations at hand. On the left, a basic element is shown with a locking ring but without a snapping mechanism for the secure locking of the ring. On the right, a design is presented with a snapping mechanism, showing the distances from the top of the element to the magnetic ring in different stages of the locking process.

easily assembled after printing due to the lack of need for overhanging angles. Therefore, the modular design allows for flexibility in adding or removing components and experimenting with them (Supplementary video 1) such that different configurations can be explored (Fig. 2c). This leads to a vast number of design possibilities, each of which can be transformed into multiple shapes. The key dimensions of the system, for both the modular design and its developments, are illustrated in Fig. 2d.

Given that magnetic fields generally have limited strength and reach and to ensure the effective operation of the snapping mechanism, it is important to minimize the required force F applied by the magnetic field on the locking ring. This force is dependent on various factors, including the properties of the magnet, the properties of the ring material, and the friction within the system. The snapping mechanism should keep the lock in place even after the removal of the magnetic stimulus and allow for the release of the lock upon the application of another activation stimulus. To achieve this, it is important to consider the potential for the magnetic field to pull the ring through the snap in two directions. We analyzed the repeatability of the process through the calculation of the

Table 1
The materials and manufacturing techniques used for designing components. The table provides information regarding the properties and limitations of each component, aiding in the determination of its suitability for the intended application.

	grey (ring)	white	transparent
material	Composite Iron PLA[a]	PLA white[b]	VeroClear (RGD810)[c]
method	MEX-TRB/P	MEX-TRB/P	MJT-UV/P
printer	Ultimaker 2+[b]	Ultimaker 2+[b]	PolyJet, ObjetJ735 Connex3[c]
layer height	0.060 mm	0.060 mm	0.027 mm
nozzle size	0.250 mm	0.250 mm	–

[a] Proto-pasta, ProtoPlant Inc., USA.
[b] Ultimaker BV, The Netherlands.
[c] Stratasys Ltd., USA.

decay $\overline{\mathscr{D}}$ associated with the lock and release cycles. This decay was calculated for both the locking and releasing processes and was defined as $\overline{\mathscr{D}} = |(F_1 - F_2)/F_1|$, where the subscripts indicate the cycle. As many parameters interact with each other, an experimental approach was used to evaluate the different designs in terms of the performance of their snapping mechanism. Four different designs (Fig. 3a) were fabricated and were subjected to uniform experimentation. All designs rely on compliant deformation of the parts to snap into place. The test samples comprised simplified versions of the design, with the removal of the redundant components. As shown in Table 1, the locking ring was printed in grey polymer with thermally bonded material extrusion of polymer (MEX-TRB/P [40]) and the other part was with material jetting of polymer with UV curing (MJT-UV/P [40]). The specimens featured enlarged, flat heads with a through hole for easy attachment to the pin grips of a testing machine (Fig. 3b-c). A Lloyd LR5K mechanical testing machine was employed to lock and release the specimens, and the applied force was measured using a 100 N load cell (Fig. 3d). Quasi-static uniaxial compression and tensile tests were conducted under displacement control at a rate of 1 mm/min until locking and releasing were achieved for each mechanism. The machine recorded the force F, displacement δ, and time (with an average sampling rate of 5 Hz) for each test. Three specimens were evaluated for each design, undergoing two cycles of locking and releasing.

The initial unit cell design enabled the formation of a larger network through structured organization in a grid. This resulted in an in-plane shape-morphing structure that could be securely locked. The unit cell design also facilitated the customization of the number of bodies in the network, allowing for close conformity to the contours of a desired shape by adjusting the position of the edge bodies. Furthermore, the internal bodies provided support to maintain the structure's shape and resist any external loads or stress. Therewith, the network design provided versatility and adaptability to different shapes, while ensuring the structural integrity and stability of the structure.

The subsequent (primarily transparent) designs that incorporate the unit cells in a grid were variations of the modular design, but they were manufactured using a different approach. The design of these specimens is presented in Fig. 2d. The grey iron composite ring was manufactured using MEX-TRB/P [40], whereas the transparent components were printed using MJT-UV/P [40] (Table 1). The MJT-UV/P [40] is a 3D printing process in which multiple streams of UV-curable polymers are

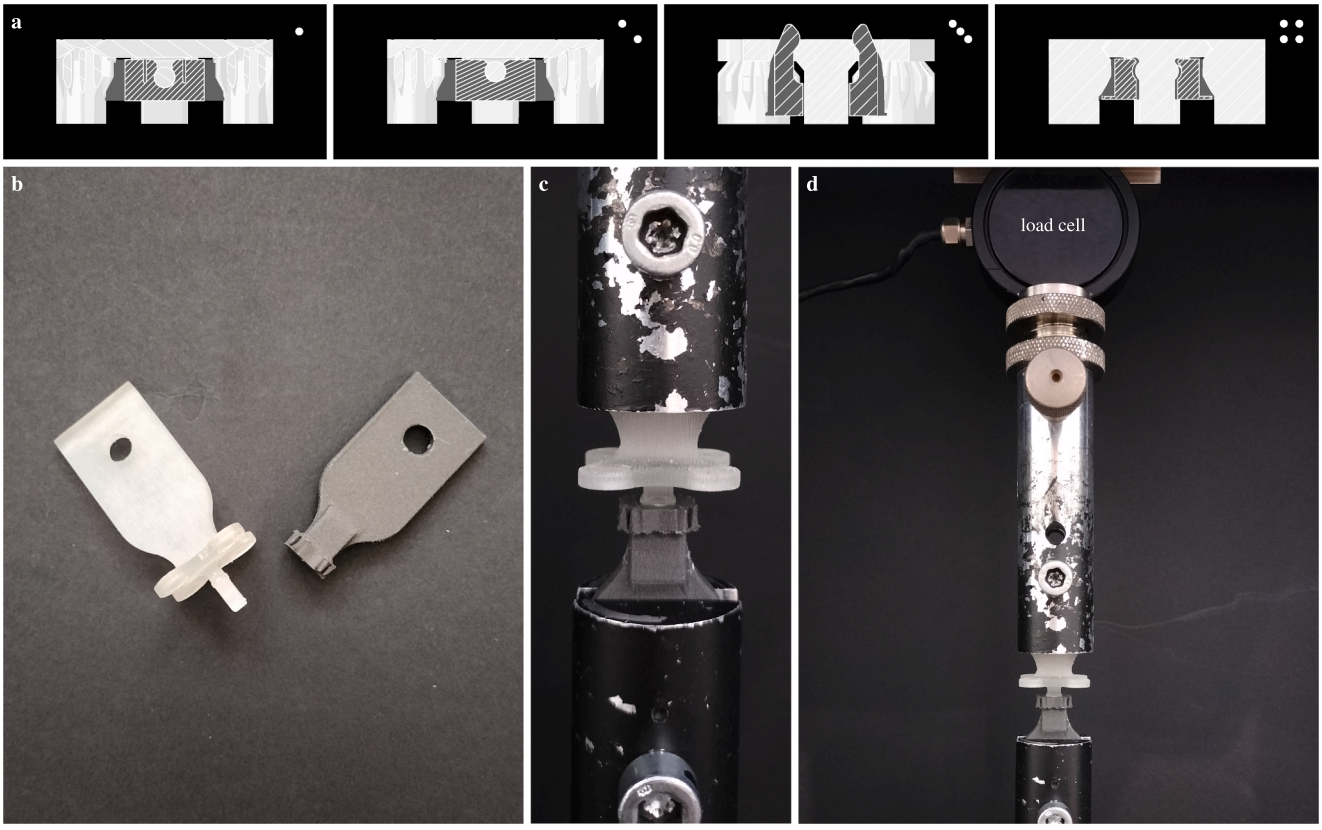

Fig. 3. The evaluation of the snapping mechanisms using a mechanical test setup to determine the required forces of the mechanism. a) Four examples, 1 to 4, of the different designs of the snapping mechanism to secure the lock in the locked position, after being pulled by a magnetic field. b) One of the four designs (specimen "4") with the notch on the transparent part and the locking ring on the grey part. c) The specimen was initialized for the test with either part placed in one of the mounts. The locking ring was placed in the immobile lower mount, while the transparent part was placed in the moving upper mount. d) The upper part moved down for locking and up for release, as the load cell measured the applied force. The load cell was connected to the upper mount and provided quantifiable data regarding the performance of the design by measuring the force required to lock the mechanism.

selectively deposited at each spatial location, and has the potential to produce the entire structure with a grid of unit cells in a single step, potentially resulting in a non-assembly design [41]. The precise tolerances this printing also enabled the creation of functioning revolute joints, given that the design accounted for the limitations of the printing process. For example, with an overhanging angle >45° (measured with respect to the horizontal plane), an integrated joint can be printed without a need for an assembly step. The non-assembly design has advantages in terms of structural integrity and reduced manufacturing time. However, in the case of the present design, the components that hold the locking ring require assembly, since the locking ring must be made of a different material. Consequently, the main grid along with the

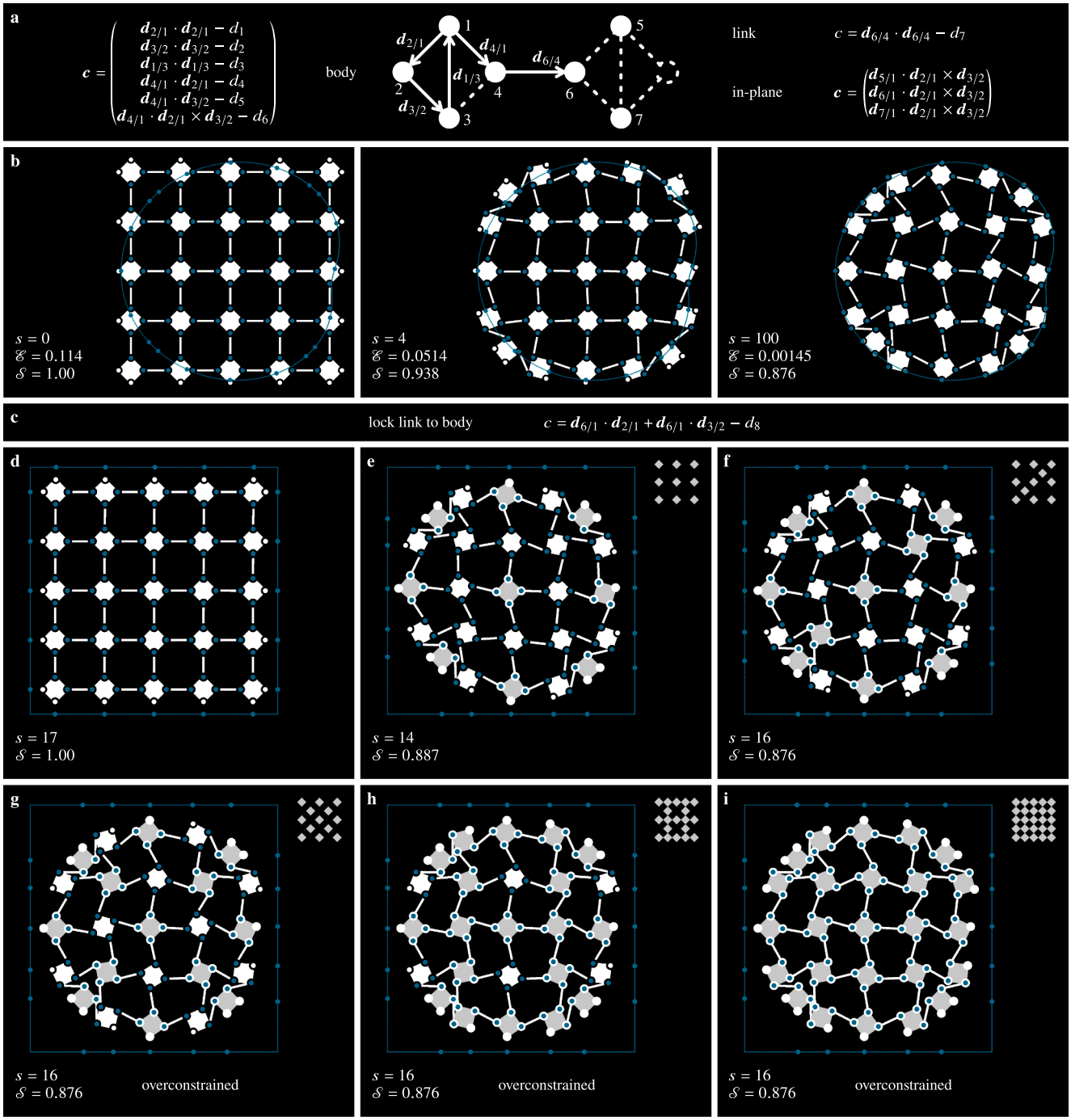

Fig. 4. Simulation of shape-morphing and shape-locking using a multibody kinematic system approach and different distributions of actively locked elements. a) Nodes (white circles) and constraints $\boldsymbol{c}$, comprised of vectors $\boldsymbol{d}$ and constants d, define the structure. b) Combining a sufficient number of these nodes and constraints results in a network of rigid bodies (white squares) and rigid links (white lines) connected via hinges. Each simulation proceeds through multiple steps, s, during which the peripheral nodes move toward the desired shape (green line), minimizing the distance error $\mathscr{E}$ between the node and the nearest point (green dot) on the target shape. A shape factor $\mathscr{S}$ was introduced to quantify the current shape relative to its initial shape. The position of nodes at various steps in this process are depicted. c) After the deformation, DoF were removed by applying additional constraints at specific locations. d)-i) Final states in an effort to return the structure to its original state, using a square target shape and altering the distribution of the locked bodies (grey squares). A locked body restricted all its attached links from rotating relative to that specific body which, in certain instances, may result in an over-constrained system. (For interpretation of the references to colour in this figure legend, the reader is referred to the web version of this article.)

revolute joints were printed without the "caps" on the bodies. The separately MEX-TRB/P [40] printed locking rings were then inserted into the bodies after which they were sealed with the caps. This approach provides opportunities to experiment with different morphing and locking mechanisms.

To further explore the versatility of the basic design, the original network structure was modified to enable morphing toward shapes that extend beyond 2D. Multiple layers of the in-plane deforming structure were combined by changing only one unit cell. The layers were connected only at their center which allowed the bodies on the edges to move independently among layers. Each layer could, therefore, be deformed and locked independently of other layers. The morphing process involved shaping the first layer into a target shape and locking it in place. Next, a connecting piece was used to stack the second layer on top of the first one, which in turn was shaped and locked into the target shape at that height. This process was repeated until the desired 3D shape was being approached through a large enough number of stacked layers.

2.2. Simulation of the locking behaviour

The complexity and interconnections of a network configuration make an analysis of the motions it can undergo non-trivial. One could determine the number of DoF through a combination of physical reasoning and calculations that take into account the number of independent constraints [42]. In our previous study [43], we developed a multibody kinematic approach aimed at analyzing the shape-morphing behaviour of mechanical metamaterials. Using this approach, the structure can be discritized into a series of nodes (or joints), bodies and links. By modifying the DoF between each node through application of independent constraints, the motion of individual elements relative to one another can be analyzed. This methodology serves as a predictive tool for the final shape of the structure.

Here, we have further extended this model to include toggling the fixation of DoF. This addition allows for the complete locking of the structure once it has morphed into a desired shape. Our analysis identified the minimum number of active elements and their optimal distribution required to fully lock the deformed structure.

The definition of the structure has case-specific characteristics to which we apply the general morphing algorithm. We assumed that all the bodies in the structure were composed of four nodes, representing the joints (or hinges) between the bodies and the links (Fig. 4a). These nodes were algebraically constrained to one another through constraints $\boldsymbol{c}$ with vectors $\boldsymbol{d}$ and constants d, facilitating either relative motion or fixed positioning between them. We constrained the out-of-plane movements of the structure, forcing it to deform only within a 2D plane. This construct of nodes and constraints was extended to a larger network to produce a 2D mesh consisting of 25 unit cells (Fig. 4b).

Subsequently, the morphing algorithm transforms the structure by repositioning the nodes. All the nodes can translate with respect to a target shape, but the nodes are limited by the constraints in the possible translations they can undergo with respect to each other. The peripheral nodes at the boundaries of the structure were selected to move toward a target shape (Fig. 4b). The target shape was created to be a dented circle to show that an initial square structure can deform into a circular shape that is not per se symmetrical. Non-peripheral nodes were allowed to move only if necessitated by the new positioning of the boundary nodes. To move the nodes, first all the possible linear motions of the nodes $\mathbf{U}$ were calculated by solving $\mathbf{JU}=\mathbf{0}$, where $\mathbf{J}$ is the Jacobian of the constraints $\boldsymbol{c}$. The morphing process then selects the allowed linear motions and superpositions them on the node locations to translate them towards new coordinates for all the nodes $\boldsymbol{x}_*$ that resembles the target shape better by using $\boldsymbol{x}_*=\boldsymbol{x}+\mathbf{U}((\mathbf{U}^\mathrm{T}\mathbf{U})^{-1}\mathbf{U}^\mathrm{T}(\boldsymbol{x}_\mathrm{g}-\boldsymbol{x}))$, where $\boldsymbol{x}$ holds all the current coordinates of the nodes and $\boldsymbol{x}_\mathrm{g}$ does the same for the target coordinates of the nodes. Therewith, the distance error $\mathscr{E}$ that represents the Euclidean distance between the deformed structure and the target location of the nodes was minimized by repositioning the nodes. Because the movements of the nodes are linear, the constraints may be violated after a movement. This was corrected with a Gauss-Newton algorithm by applying $\boldsymbol{x}=\boldsymbol{x}_*-\mathbf{J}^\mathrm{T}(\mathbf{J}\mathbf{J}^\mathrm{T})^{-1}\boldsymbol{c}$ until the constraints are satisfied within the chosen tolerance. This whole process required several iterations over multiple steps s to come to a point where $\mathscr{E}$ settles on a constant minimum value. To assess the shape, we introduced a parameter called shape factor $\mathscr{S}$ that measures the average distance of all the nodes from their collective geometrical centroid. This parameter, therefore, provides a quantitative metric for comparing various shapes.

To lock parts of the structure, we developed and applied additional constraints (Fig. 4c). Specifically, nodes were locked in groups of four per body, thereby imposing four extra constraints and removing four DoF around a body.

Given the presence of multiple bodies and joints in a closed loop, it is unnecessary to lock every joint to fully lock the deformed structure. Our multibody kinematic system approach, involving varying distributions of active elements (Fig. 4d-i) showed that even with not all the elements individually locked, still all DoF can be constrained. The absence of active elements enables the structure to return to its original configuration (Fig. 4d). However, converting all passive joints into active ones resulted in an over-constrained system, introducing singularities in our model (Fig. 4i). Hence, our multibody kinematic system approach provides a platform to rationally distribute active elements within the structure, making it possible to fully lock the system without introducing redundant constraints (Fig. 4f).

3. Results and discussion

Physical locking and releasing experiments were performed to gather information on the maximum required snapping forces and the force decay for the four designs of the snapping mechanism (Fig. 3). The results were used to determine the maximum force required for each locking and releasing cycle and for each specimen of the four designs (Fig. 5). The collected data was analyzed to compute the average locking and releasing forces for each design, as well as the force decay between cycles. These experiments offered insights into the snapping performance and can inform the optimization of the design for specific applications. The results of the mechanical testing of the four snap designs indicated variability in the maximum required forces and force decays among the different (semi-)cycles for each design. Nevertheless, one design (i.e., design 4 where the grey locking ring has a notch that is snapped over a rim on the body) outperformed the others. The forces required for releasing were lower than for locking, which can be attributed to asymmetry in certain designs and mechanism wear after a snap for all designs. This wear sometimes caused cracks to form and parts to break in either the ring or notch components. The force decay was utilized as a measure of wear. Based on this analysis, design "4″ was selected for implementation in the structures due to its low force requirements for both locking and releasing and its average force decay. Note that the selection of design "4" is merely an indication of the best snapping design. Actual values are application-dependent and contingent upon various factors, such as dimensions, material properties (including magnetic properties), manufacturing process, locking speed (dynamics), and the strength of the magnetic field. Further optimization is, therefore, necessary to customize the design to the specific needs of any particular application.

The network structures, with their different variations, could be deformed and locked into various shapes, displaying a range of design possibilities. The simplest way to achieve this is by incorporating a locking mechanism in each individual body. By deforming the structure into a target shape and locking it with a magnet, the structure maintained its form (Fig. 6a-e and Supplementary video 2). For example, the deformed structure could support and lift a load (Fig. 6f). By attaching a connecting piece to one of the slightly modified unit cells, multiple independent layers could be stacked on top of each other, thereby offering

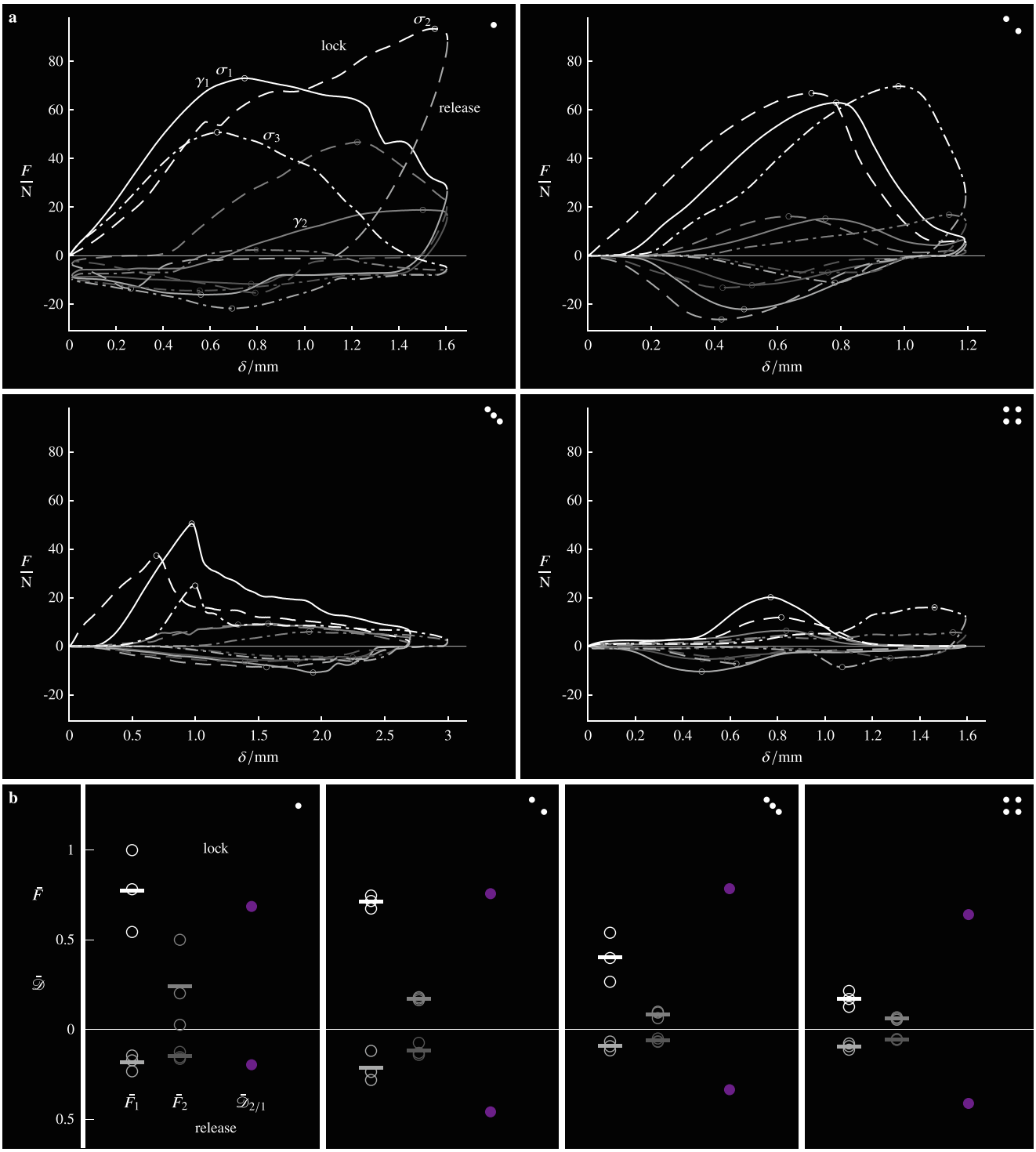

Fig. 5. The results of the mechanical tests for the snapping mechanisms of designs 1 to 4. a) Force F is plotted versus displacement δ. Three specimens σ were tested for each design and two lock/release cycles γ were performed. The maximum force values during the locking and releasing phases were determined and were plotted as open circles (units and quantities as per [44]). b) The processed results of the mechanical tests on the four designs for both cycles, 1 and 2, of locking and releasing. The absolute normalized maximum locking and releasing forces $\bar{F}$ are indicated by open circles, with the plotted bars representing the mean of these measurements. All the values are normalized with respect to the maximum measured force across all the experiments for comparison purposes. The decays $\overline{\mathscr{D}}$ in the mean required forces between the cycles are presented as purple dots. (For interpretation of the references to colour in this figure legend, the reader is referred to the web version of this article.)

the possibility to approximate 3D shapes (Fig. 7a-c). Making selective bodies passive (Fig. 7d-e) facilitates the possibility to achieve locking by activating a smaller number of cells, while keeping all the unit cells in a fixed position after locking. These passive elements were manufactured as a single piece, eliminating the need for assembly.

Locking mechanisms can be introduced into the design of specific kinematic in-plane deforming structures [8]. The specific locking mechanism introduced in the current study utilizes magnetism to

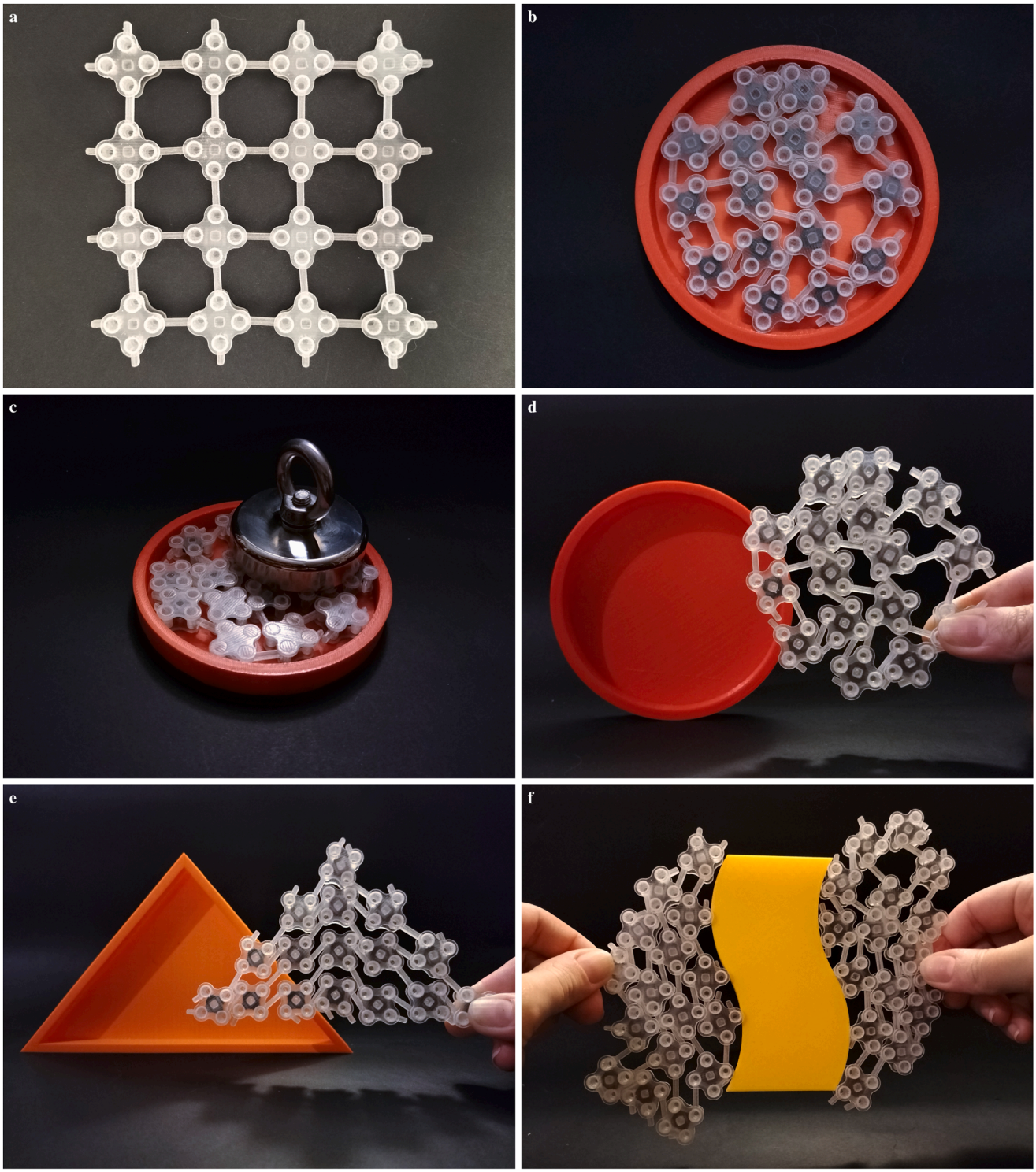

Fig. 6. The final design of the in-plane shape morphing magnetic locking structures. The structure included ferromagnetic locking rings (MEX-TRB/P [40]) that are depicted in grey and transparent elements (MJT-UV/P [40]). a) The assembled structure prior to morphing. b) The structure after morphing into a circular shape. c) Shape locking was achieved by a magnetic field. d) The locked structure maintains its acquired shape. e) Different target shapes, such as a triangle, can also be attained. f) A potential application is the grasping of objects.

mechanically block the rotation of revolute joints and lock the system in place (Figs. 2 and 6 and Supplementary video 1–2). This enables non-contact shape locking, which are particularly important in such applications as implantable medical devices where shape locking may need to be realized during the surgery in which case the non-contact nature of our proposed technique can both minimize the invasiveness of the surgical procedure and reduce the risk of bacterial infections. While the proposed principle has the potential for various practical applications beyond implantable devices, it also serves as a representative example to study the general features of locking mechanisms in shape morphing structures. We, therefore, investigated morphing and locking mechanisms and studied how the current design fits into those considerations.

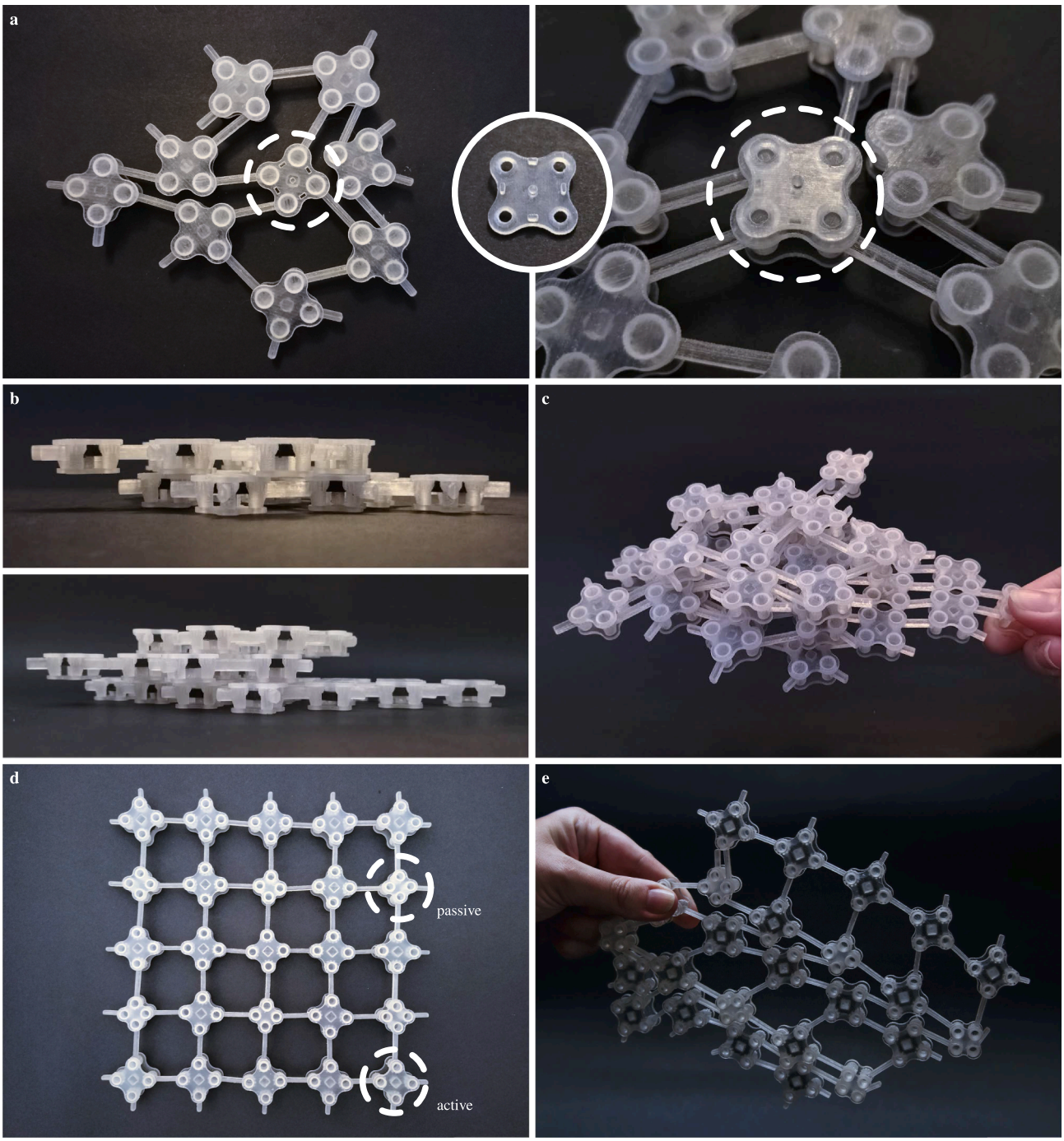

Fig. 7. Design additions to the basic design. a) Stacking multiple layers enhances the morphing capabilities of the structure, allowing for the approximation of certain types of 3D shapes. An insert piece was attached to the center element of the first layer, which has been morphed and locked. b) A second layer was attached to the first one and underwent similar morphing and locking processes. Additional layers can be added if necessary. c) Each layer can be morphed and locked independently, resulting in a stable fixation. d) Removing redundant constraints after locking by a combination of active locking elements and passive elements that do not possess any locking elements. e) The DoF of the structure can all still be locked.

3.1. Activation energy

Activation mechanisms are necessary for controlling the shape morphing and shape locking capabilities of a structure. These mechanisms can be powered by various energy sources or a combination of them. The choice of the activation method has a significant impact on the performance of the structure. It also determines the reversibility and repeatability of the shape morphing and locking processes, as well as whether they can be applied locally or globally. It is important to note that shape-morphing itself can function as a form of self-locking, as demonstrated by such examples as a spring-tensioned array of kinematic joints pushed into a cavity, which maintains its shape by exerting pressure against the object [8].

Here, the locking mechanism is mechanical and uses magnetism for activation (Fig. 2a-c). This mechanism works by applying a magnetic field perpendicular to the plane of the structure, which pulls a piece into place that blocks the rotation of the joints. Although this design has limitations in its in-plane deforming capabilities, it makes it easier to apply a unidirectional magnetic field to activate the lock. The loads on the structure are solely related to the activation force required to lock

the system by means of friction forces. Magnetic locking offers potential advantages, including non-contact activation from a distance and the ability to locally manipulate the shape of the structure [32]. In applications where a strong magnetic field can be used, the design can be implemented as is, for example to fill 2D holes. In other applications, such as (soft) robotics, the lock activation can be performed both on-board the structure by integrating electromagnets that can move the magnetic ring between the lock and release position and remotely through external magnetic fields. The performance of the mechanism depends on the strength of the magnetic field and the magnetic properties of the part being manipulated.

3.2. Reversibility and repeatability

The morphing and locking processes can be reversed, allowing the structure to return to its initial state. Given that this cycle can occur multiple times, it is referred to as a repeatable process. While in some applications, such as shape-morphing orthopedic implants, permanent locking is required, some other applications, such as robotics, require reversible and repeatable locking. The reversibility and repeatability of the locking mechanism is dependent on the activation energy required and its implementation in a specific design. The design also determines whether the reversal process occurs passively (i.e., through removal of the initial stimulus) or actively (i.e., through the application of a second stimulus).

The proposed designs exhibit both reversibility and repeatability in their shape morphing and shape locking behaviors. The reversal process can occur passively or actively, depending on whether a snapping mechanism is present in the locking mechanism. In the absence of a snapping mechanism, the lock can be released by removing the magnetic stimulus, either due to gravity or by implementing a spring, making it independent of the orientation of the structure. When a snapping mechanism is present, the lock must be released by applying a magnetic stimulus in the opposite direction. Following the release of the lock, the structure can be transformed and locked again. These processes can be repeated multiple times, although repeated use may induce wear as suggested by the diminishing snapping forces depicted in Fig. 5.

3.3. Selective locking

Selective locking refers to the ability to restrict or manipulate the motion of a structure by constraining specific joints or DoF rather than affecting the motion of the entire structure. The optimal method of constraining depends on the application. In the case of implantable devices, for instance, it is advisable to ensure maximum stability by completely locking the mechanism using a minimum number of locking elements [8]. In soft robotics, however, it may be beneficial to have selected region locking, allowing certain regions of the structure to deform easily while other regions remain locked.

The current design locks the joints in groups of four per body. The magnetic field can be manipulated and directed to lock several or all joints. This localized behavior is also applicable to the manipulation of individual body positions.

The simulated findings of making elements passive and removing redundant constraints (Fig. 4d-i) were implemented in a physical design (Fig. 7d-e). Indeed, not all elements need to be locked to remove all DoF from a structure. This approach reduced the complexity of activation. However, it also limited the options for selective locking and decreased the locking strength as compared to the case where redundant constraints were used. In physical implementations, the strength of the locked structure decreases as passive elements are introduced. The redundant constraints contribute to the maintenance of the structural integrity and could result in a more stable load bearing structure. Therefore, adding too many passive elements without this consideration is suboptimal. One of the benefits of using passive elements, especially those made of a single material, is the feasibility of fabricating the structure using efficient, non-assembly manufacturing techniques, such as via MJT-UV [40] printing technology, which could lead to reduced manufacturing costs.

3.4. Continuity

The locking of a morphing structure can be applied at specific stages of the morphing process or continuously to any arbitrary shape of the structure. A ratchet system, for example, has discrete steps at which the position is fixed. To eliminate these steps, a mechanism that operates with deforming materials or friction can be incorporated.

The mechanical lock in the presented designs is based on the discrete blocking of a joint. The teeth of the non-rotating ring engage with those of the struts ends. This lock is more straightforward and easier to implement than a friction lock, but it has the disadvantage of having a limited number of discrete locking positions. This may constrain the range of the shapes and positions that the structure can assume. This design, however, also offers the advantage of being more reliable and easier to control than a friction-based lock, since it is less impacted by external factors, such as temperature and humidity.

3.5. Applications, design, and manufacturing

Shape-morphing and locking structures can be applied across a diverse range of research areas from biomedical engineering (e.g., orthopedic implants and exoskeletal suits), to both soft and conventional robotics, and the design of gripping systems. Within the domain of medical implants, these advanced structures facilitate the creation of adaptive implants specifically engineered to integrate seamlessly with the human anatomy [1,2]. This enhances not only patient comfort but also the functional efficacy of the implants and prosthetic devices. Moreover, exosuits, integrated with shape morphing technologies, offer ergonomic and mechanically efficient support for human locomotion. These suits find diverse applications ranging from physical rehabilitation and augmentation to specialized industrial tasks [3]. In the robotics sector, shape-morphing technologies endow robots with the capacity to dynamically adapt their shape, thereby enhancing their functional capabilities in terms of locomotion, manipulation, and overall versatility [4–7]. Soft robotics, in particular, can benefit from these advanced structures, as they enable more secure and nuanced interactions with delicate objects (e.g., human soft tissue) [5]. This expansion in interaction modalities consequently broadens the scope for human-robot interactions, for example, in minimally invasive surgeries [5]. Regarding robotic grippers, the incorporation of shape-morphing and locking materials into such devices provides them an ability to grasp a wide range of objects regardless of their varied shapes and sizes [4]. This capability is particularly valuable in industrial contexts that require flexible automation strategies. It should be noted that the applicability of shape-morphing structures is not limited to the aforementioned categories. The design of these structures can be precisely tailored to optimize performance across a myriad of applications, suggesting new horizons for developing smart materials with multiple functionalities.

The design and manufacturing choices play a significant role in determining the performance of a mechanism. For instance, not all the joints in a network need to be hinges to ensure planar deformation. Cleverly alternating between hinges and spherical joints can ensure the desired deformation behavior is achieved while preventing self-stress in the structure as much as possible. Reduction in the number of locked elements as presented here is a first step toward optimization for reducing self-stress. Further and more sophisticated mechanical analyses using finite element models combined with optimization algorithms could further enhance the design in terms of minimizing self-stresses and is suggested as an avenue of future research. Another example is that a morphing structure with many DoF and smaller components will generally perform better in reaching a target shape. Different manufacturing methods that use various materials result in

different characteristics, including dimensions, weight, resolution, tolerance, surface roughness, friction, wear, biocompatibility, and ease of operation and processing. These characteristics can be fine-tuned to satisfy the specific requirements associated with any application.

This work aimed at demonstrating the concept of locking a kinematically deforming mechanism, rather than optimizing it for a specific application. To this end, the structures were made as small as possible using available 3D printing techniques (Table 1). While (some of) the proposed designs are manufacturable using other fabrication approaches, AM provides additional flexibility, lower costs, and shorter lead times that make it easier for researchers to experiment with different designs. AM also has the potential to be used for an end product because non-assembly AM approaches could circumvent much of the challenges associated with the assembly of large kinematic structures made using other techniques. The post-processing required for the MEX-printed parts was minimal, while MJT printed parts required more extensive post-processing. It was observed that the friction between the locking ring and the MEX printed parts was less than the one between the locking ring and MJT printed parts, possibly due to differences in their surface roughness. The selected design presents some limitations in terms of its morphing capabilities, as it can only deform in-plane. Nonetheless, stacking multiple layers can approximate 3D target shapes (Fig. 7a-c). The manufacturing techniques were selected based on the ease of experimentation, which is why 3D printing was used. Ideally, the designs would be non-assembly. Given the current state of 3D printing technology, this is only possible for specific parts of the designs. That is because the application of the magnetic fields requires differential magnetic responses in the 3D printed materials. This calls for the simultaneous printing of magnetic and non-magnetic materials. Moreover, the clearances required for the kinematic joints necessitate the use of a solvent-soluble or otherwise removable support material. There are currently no readily available multi-material 3D printing techniques that can simultaneously print all these materials with sufficient quality and resolution to enable smooth functioning of both shape morphing and shape locking mechanisms. While we were successful in removing many of the otherwise required assembly steps, there were still a few assembly stages that were needed for incorporating all the printed materials and components.

To improve the manufacturing of the structures, alternative methods and materials, such as powder bed fusion of metal using a laser beam (PBF-LB/M [40]), could be employed. PBF-LB/M [40] has a resolution that varies with the granulometry of the powder used and the laser spot size and is typically in the 0.01 mm to 0.1 mm range. It also enables the use of both magnetic and non-magnetic powders (e.g., iron, nickel, or cobalt alloys), although most printers can print only one material at a time. Other extrusion-based metal printing techniques may offer the potential for multi-material printing and the use of biocompatible magnetic materials [45,46]. Another avenue for improvement is the development of multi-material 3D printing on a small scale, which would enable the creation of an integrated, non-assembly structure. Further improvements in material selection, geometry, and dimensions could lead to the creation of alternative configurations with the same basic conceptual design and functionality. For a magnetism-based mechanism as presented here, we need a non-magnetic as well as a magnetic material. The composition of these materials can be polymer-based, as used here, or fully metallic if AM techniques allow it [47]. Numerical simulation serves as a pivotal tool in optimizing the design of these structures, as demonstrated through the kinematic analysis presented in Fig. 4. Additional computational models may be utilized, for example, to predict the overall strength of the structure. In all these choices, it is essential to emphasize that the primary goal of locking is to stiffen the structure, enabling it to maintain its shape and support the loads it experiences as required by the design objectives.

4. Conclusions

In this study, we presented the implementation of a magnetic locking mechanism in a shape morphing structure to support loads. The kinematic structure, which deforms in-plane, has revolute joints that are mechanically locked using magnetism. We utilized two additive manufacturing methods to fabricate prototypes of the conceptual designs. We also evaluated the mechanical performance of the locking mechanism and demonstrated its application in a closed-loop grid and showed how the activation effort can be reduced through design iterations. Furthermore, we extended the design of the proposed mechanism and demonstrated its applicability for certain types of 3D encapsulations by stacking in-plane structures. Our study highlights the feasibility of a locking concept and provides insight into design considerations for the locking mechanisms. It also offers a methodology for analyzing the kinematics of the system through simulation. With further improvements and optimization, the designs presented here may have the potential for broader applications in such fields as robotics, architecture, and biomedical engineering. The design can be further enhanced and optimized to increase its efficiency and effectiveness.

Declaration of Competing Interest

The authors declare that they have no known competing financial interests or personal relationships that could have appeared to influence the work reported in this paper.

Data availability

Data will be made available on request.

Acknowledgments

This work is part of the research program: “Metallic clay: shape-matching orthopaedic implants” with project number 16582, which is financed by the Dutch Research Council (NWO), The Netherlands. The Authors would like to thank Mauricio Cruz Saldivar for his support, specifically but not exclusively, by deploying the PolyJet.

Appendix A. Supplementary data

Supplementary data to this article can be found online at https://doi.org/10.1016/j.matdes.2023.112427.

References

[1] H.M.A. Kolken, S. Janbaz, S.M.A. Leeflang, K. Lietaert, H.H. Weinans, A. A. Zadpoor, Rationally designed meta-implants: a combination of auxetic and conventional meta-biomaterials, Mater. Horiz. 5 (1) (2018) 28–35, https://doi.org/10.1039/C7MH00699C.
[2] M.J. Mirzaali, S. Janbaz, M. Strano, L. Vergani, A.A. Zadpoor, Shape-matching soft mechanical metamaterials, Sci Rep 8 (1) (2018) 965, https://doi.org/10.1038/s41598-018-19381-3.
[3] A.F. Pérez Vidal, et al., Soft exoskeletons: development, requirements, and challenges of the last decade, Actuators 10 (7) (2021) 166, https://doi.org/10.3390/act10070166.
[4] J. Shintake, V. Cacucciolo, D. Floreano, H. Shea, Soft robotic grippers, Adv. Mater. 30 (29) (2018) 1707035, https://doi.org/10.1002/adma.201707035.
[5] T. Ashuri, A. Armani, R. Jalilzadeh Hamidi, T. Reasnor, S. Ahmadi, K. Iqbal, Biomedical soft robots: current status and perspective, Biomed. Eng. Lett. 10 (3) (2020) 369–385, https://doi.org/10.1007/s13534-020-00157-6.
[6] N. El-Atab, et al., Soft actuators for soft robotic applications: A review, Adv. Intell. Syst. 2 (10) (2020) 2000128, https://doi.org/10.1002/aisy.202000128.
[7] F. Ahmed, et al., Decade of bio-inspired soft robots: a review, Smart Mater. Struct. 31 (7) (2022), 073002, https://doi.org/10.1088/1361-665X/ac6e15.
[8] S. Leeflang, S. Janbaz, A.A. Zadpoor, Metallic clay, Add. Manuf. 28 (2019) 528–534, https://doi.org/10.1016/j.addma.2019.05.032.
[9] S. Kamrava, D. Mousanezhad, H. Ebrahimi, R. Ghosh, A. Vaziri, Origami-based cellular metamaterial with auxetic, bistable, and self-locking properties, Sci Rep 7 (1) (2017) 46046, https://doi.org/10.1038/srep46046.

[10] J. Troutner *et al.*, "Orthopedic support apparatus and method of use," US20180153745A1, Jun. 07, 2018 Accessed: Dec. 20, 2022. [Online]. Available: https://patents.google.com/patent/US20180153745A1/en.
[11] M. Behl, K. Kratz, J. Zotzmann, U. Nöchel, A. Lendlein, Reversible Bidirectional Shape-Memory Polymers, Adv. Mater. 25 (32) (2013) 4466–4469, https://doi.org/10.1002/adma.201300880.
[12] X. Chen, et al., Multi-metal 4D printing with a desktop electrochemical 3D printer, Sci Rep 9 (1) (2019) 3973, https://doi.org/10.1038/s41598-019-40774-5.
[13] R.M. Erb, J.S. Sander, R. Grisch, A.R. Studart, Self-shaping composites with programmable bioinspired microstructures, Nat Commun 4 (1) (2013) 1712, https://doi.org/10.1038/ncomms2666.
[14] M. Mehrpouya, H. Vahabi, S. Janbaz, A. Darafsheh, T.R. Mazur, S. Ramakrishna, 4D printing of shape memory polylactic acid (PLA), Polymer 230 (2021), 124080, https://doi.org/10.1016/j.polymer.2021.124080.
[15] T. van Manen, S. Janbaz, A.A. Zadpoor, Programming 2D/3D shape-shifting with hobbyist 3D printers, Mater. Horiz. 4 (6) (2017) 1064–1069, https://doi.org/10.1039/C7MH00269F.
[16] T. van Manen, S. Janbaz, K.M.B. Jansen, A.A. Zadpoor, 4D printing of reconfigurable metamaterials and devices, Commun Mater 2 (1) (2021) 56, https://doi.org/10.1038/s43246-021-00165-8.
[17] H. Wei, Q. Zhang, Y. Yao, L. Liu, Y. Liu, J. Leng, Direct-write fabrication of 4D active shape-changing structures based on a shape memory polymer and its nanocomposite, ACS Appl. Mater. Interfaces 9 (1) (2017) 876–883, https://doi.org/10.1021/acsami.6b12824.
[18] J. Wu, et al., Multi-shape active composites by 3D printing of digital shape memory polymers, Sci. Rep. 6 (1) (2016) 24224, https://doi.org/10.1038/srep24224.
[19] B. Gorissen, D. Reynaerts, S. Konishi, K. Yoshida, J.-W. Kim, M. De Volder, Elastic inflatable actuators for soft robotic applications, Adv. Mater. 29 (43) (2017) 1604977, https://doi.org/10.1002/adma.201604977.
[20] Y. Alapan, A.C. Karacakol, S.N. Guzelhan, I. Isik, M. Sitti, Reprogrammable shape morphing of magnetic soft machines, Sci. Adv. 6 (38) (2020), https://doi.org/10.1126/sciadv.abc6414.
[21] A.K. Bastola, M. Hossain, The shape – morphing performance of magnetoactive soft materials, Materials & Design 211 (2021), 110172, https://doi.org/10.1016/j.matdes.2021.110172.
[22] T. Chen, et al., Harnessing magnets to design tunable architected bistable material, Adv. Eng. Mater. 21 (3) (2019) 1801255, https://doi.org/10.1002/adem.201801255.
[23] E. Diller, J. Zhuang, G. Zhan Lum, M.R. Edwards, M. Sitti, Continuously distributed magnetization profile for millimeter-scale elastomeric undulatory swimming, Appl. Phys. Lett. 104 (17) (2014), 174101, https://doi.org/10.1063/1.4874306.
[24] K.G., B. Kandasubramanian, Exertions of magnetic polymer composites fabricated via 3D printing, Ind. Eng. Chem. Res. 61 (46) (2022) 16895–16909, https://doi.org/10.1021/acs.iecr.2c02299.
[25] Y. Kim, H. Yuk, R. Zhao, S.A. Chester, X. Zhao, Printing ferromagnetic domains for untethered fast-transforming soft materials, Nature 558 (7709) (2018) 274–279, https://doi.org/10.1038/s41586-018-0185-0.
[26] G.Z. Lum, et al., Shape-programmable magnetic soft matter, Proc. Natl. Acad. Sci. USA 113 (41) (2016), https://doi.org/10.1073/pnas.1608193113.
[27] S.J.M. van Vilsteren, H. Yarmand, S. Ghodrat, Review of magnetic shape memory polymers and magnetic soft materials, Magnetochemistry 7 (9) (2021) 123, https://doi.org/10.3390/magnetochemistry7090123.
[28] X. Wang, et al., Untethered and ultrafast soft-bodied robots, Commun Mater 1 (1) (2020) 67, https://doi.org/10.1038/s43246-020-00067-1.
[29] Q. Hu, H. Huang, E. Dong, D. Sun, A bioinspired composite finger with self-locking joints, IEEE Robot. Autom. Lett. 6 (2) (2021) 1391–1398, https://doi.org/10.1109/LRA.2021.3056345.
[30] A.T. Clare, P.R. Chalker, S. Davies, C.J. Sutcliffe, S. Tsopanos, Selective laser melting of high aspect ratio 3D nickel–titanium structures two way trained for MEMS applications, Int. J. Mech. Mater. Des. 4 (2) (2008) 181–187, https://doi.org/10.1007/s10999-007-9032-4.
[31] J. Tang, et al., Super tough magnetic hydrogels for remotely triggered shape morphing, J. Mater. Chem. B 6 (18) (2018) 2713–2722, https://doi.org/10.1039/C8TB00568K.
[32] J. Tang, Q. Yin, Y. Qiao, T. Wang, Shape morphing of hydrogels in alternating magnetic field, ACS Appl. Mater. Interfaces 11 (23) (2019) 21194–21200, https://doi.org/10.1021/acsami.9b05742.
[33] D.G. Chung, J. Kim, D. Baek, J. Kim, D.-S. Kwon, Shape-locking mechanism of flexible joint using mechanical latch with electromagnetic force, IEEE Robot. Autom. Lett. 4 (3) (2019) 2661–2668, https://doi.org/10.1109/LRA.2019.2897006.
[34] A.Y. Lee, J. An, C.K. Chua, Two-way 4D printing: A review on the reversibility of 3D-printed shape memory materials, Engineering 3 (5) (2017) 663–674, https://doi.org/10.1016/J.ENG.2017.05.014.
[35] M. Plooij, G. Mathijssen, P. Cherelle, D. Lefeber, B. Vanderborght, Lock your robot: A review of locking devices in robotics, IEEE Robot. Automat. Mag. 22 (1) (2015) 106–117, https://doi.org/10.1109/MRA.2014.2381368.
[36] K. Bertoldi, V. Vitelli, J. Christensen, M. van Hecke, Flexible mechanical metamaterials, Nat Rev Mater 2 (11) (2017) 17066, https://doi.org/10.1038/natrevmats.2017.66.
[37] A. Valipour, M.H. Kargozarfard, M. Rakhshi, A. Yaghootian, H.M. Sedighi, Metamaterials and their applications: An overview, Proc. Inst. Mech. Eng., Part L: J. Mater. Design Appl. (2021), https://doi.org/10.1177/1464420721995858.
[38] F.S.L. Bobbert, S. Janbaz, A.A. Zadpoor, Towards deployable meta-implants, J. Mater. Chem. B 6 (21) (2018) 3449–3455, https://doi.org/10.1039/C8TB00576A.
[39] M.A. Leeflang, F.S.L. Bobbert, A.A. Zadpoor, Additive manufacturing of non-assembly deployable mechanisms for the treatment of large bony defects, Add. Manuf. 46 (2021), 102194, https://doi.org/10.1016/j.addma.2021.102194.
[40] ISO and ASTM, "52900 Additive manufacturing - General principles - Fundamentals and vocabulary." Nov. 2021.
[41] K. Lussenburg, A. Sakes, P. Breedveld, Design of non-assembly mechanisms: A state-of-the-art review, Add. Manuf. 39 (2021), 101846, https://doi.org/10.1016/j.addma.2021.101846.
[42] J. Wittenburg, *Kinematics*. Berlin, Heidelberg: Springer Berlin Heidelberg, 2016. 10.1007/978-3-662-48487-6.
[43] P.H. de Jong, A.L. Schwab, M.J. Mirzaali, A.A. Zadpoor, A multibody kinematic system approach for the design of shape-morphing mechanism-based metamaterials, Commun Mater 4 (1) (Oct. 2023) 83, https://doi.org/10.1038/s43246-023-00410-2.
[44] ISO, "80000-1 Quantities and units - Part 1: General." Dec. 2022.
[45] N.E. Putra, et al., Additive manufacturing of bioactive and biodegradable porous iron-akermanite composites for bone regeneration, Acta Biomaterialia 148 (Aug. 2022) 355–373, https://doi.org/10.1016/j.actbio.2022.06.009.
[46] N.E. Putra, et al., Poly(2-ethyl-2-oxazoline) coating of additively manufactured biodegradable porous iron, Biomater. Adv. 133 (2022), 112617, https://doi.org/10.1016/j.msec.2021.112617.
[47] X. Wei, M.-L. Jin, H. Yang, X.-X. Wang, Y.-Z. Long, Z. Chen, Advances in 3D printing of magnetic materials: Fabrication, properties, and their applications, J Adv Ceram 11 (5) (2022) 665–701, https://doi.org/10.1007/s40145-022-0567-5.